

Reliability Assessment of Nanoscale System on Chip Depending on Neutron Irradiation

*Original*

Reliability Assessment of Nanoscale System on Chip Depending on Neutron Irradiation / Yang, Weitao; Li, Yang; Hu, Zhiliang; He, Chaohui; Cai, Jiale; Wu, Longsheng. - In: ELECTRONICS. - ISSN 2079-9292. - (2023).

*Availability:*

This version is available at: 11583/2978090 since: 2023-04-21T07:04:08Z

*Publisher:*

MDPI

*Published*

DOI:

*Terms of use:*

This article is made available under terms and conditions as specified in the corresponding bibliographic description in the repository

*Publisher copyright*

(Article begins on next page)

# Reliability Assessment of Nanoscale System on Chip Depending on Neutron Irradiation

Weitao Yang<sup>a,b,c</sup>, Yang Li<sup>b</sup>, Zhiliang Hu<sup>b,c,d</sup>, Chaohui He<sup>b</sup>, Jiale Cai<sup>f</sup>, Longsheng Wu<sup>a</sup>

<sup>a</sup>School of Microelectronics, Xidian University, Xi'an 710071, China

<sup>b</sup>School of Nuclear Science & Technology, Xi'an Jiaotong University, Xi'an 710049, China

<sup>c</sup>Spallation Neutron Source Science Center, Dongguan 523803, China

<sup>d</sup>Institute of High Energy Physics, Chinese Academy of Sciences (CAS), Beijing 100049, China

<sup>e</sup>Dipartimento di Automatica e Informatica, Politecnico di Torino, Torino 10129, Italy

<sup>f</sup>Dipartimento di Elettronica e Telecomunicazioni, Politecnico di Torino, Torino 10129, Italy

The atmospheric neutron poses a serious hazard to nanoscale electronics reliability. Spallation neutron irradiations on a nanoscale system on chip (SoC) were conducted applying the China Spallation Neutron Source (CSNS), and the results were compared and analyzed using Monte Carlo simulation. The contribution from thermal neutron on the SoC single event effect (SEE) was analyzed. Analysis indicated the SoC atmospheric neutron SEE vulnerability can be reduced by 44.4% if the thermal neutron was absorbed. The influences of the B and Hf elements on the SEEs were evaluated, too. It can be concluded that  $^{10}\text{B}$  interacting with thermal neutron is the reason for thermal neutron inducing SEE in the SoC. Although the Hf element has no contribution to the 28 nm SoC atmospheric neutron SEE cross section, it increases the total dose risk 5 times during atmospheric neutron irradiation.

**Keywords:** Spallation Neutron; Monte Carlo; System on Chip; Thermal Neutron; Single Event Effect

## 1. Introduction

In 2001, Robert C. Baumann first reported  $^{10}\text{B}$  interacting with thermal neutron is a dominant factor in soft errors for deep-submicron static random access memory with borophosphosilicate glass (BPSG) packages.<sup>[1]</sup> Since then, advanced integrated circuit development makes the chip packages get rid of the BPSG package.<sup>[2-3]</sup> The nanoscale electronics, however, even though the BPSG package is not available anymore, they have to face the risk from  $^{10}\text{B}$  interacting with thermal neutron once again.<sup>[4-7]</sup> The reason is  $^{10}\text{B}$  still existing in the semiconductor contact and doping processes, and the rapidly developed semiconductor manufacturing technology pushes their supply voltages and single event effect (SEE) critical charges lower and lower.

In [6], C. Weulersse examined a variety of memories taking advantage of multi neutron sources and pointed out the related reliability problem. SEE, induced by  $^{10}\text{B}$  in nanoscale memories via interacting with thermal neutron, is even close to that caused by high energy neutrons. In [8], the 65 nm microcontroller unit (MCU) without BPSG was irradiated with thermal and high energy neutrons, and the influence of  $^{10}\text{B}$  on SEE was investigated. The results demonstrated that the contribution of  $^{10}\text{B}$  interacting with thermal neutron even dominated the atmospheric neutron SEE in the device. Specifically, the SEE ratio induced by thermal and higher energy neutrons on the 65 nm MCU reached 1.89:1.<sup>[8]</sup>

The 65 nm MCU test results signify that the interaction of  $^{10}\text{B}$  with thermal neutron is still serious to advanced integrated chips. For the 28 nm SoC, besides the boron contamination, another is also introduced: the hafnium (Hf) element. Compared with boron (B), the neutron cross section with Hf is higher at several eV intervals. Fig.1 displays the neutron cross section spectrums of  $^{10}\text{B}$ ,  $^{178}\text{Hf}$ , and  $^{28}\text{Si}$ .<sup>[9]</sup> It can be viewed the peak cross section of  $^{178}\text{Hf}$  even achieves  $10^5$  barns. The cross sections of  $^{178}\text{Hf}$  with thermal neutron are also higher than that of  $^{28}\text{Si}$  by two orders of magnitudes. Another significant fact is that the B element exists in the

27 **28 nm** SoC as the contamination from manufacturing processes, while **the Hf element** is a  
28 component of the metal gate in the **28 nm SoC**. This process makes the **28 nm** SoC atmospheric  
29 neutron SEE **evaluation** become more complicated.

30 For the **28 nm** SoC atmospheric neutron SEE, the first irradiation test **has been conducted** at  
31 **the** China Spallation Neutron Source (CSNS)-BL09.<sup>[10]</sup> In **the** irradiation, the neutron beam  
32 **hit** the chip directly without any shield, and the neutron spectrum covered **the thermal** and  
33 high energy **neutrons**. To **explore** the atmospheric neutron SEE on **the 28 nm** SoC further, the  
34 second irradiation on the SoC was performed **once more**. **But a 2 mm** cadmium (Cd) slat was  
35 used to absorb the thermal neutron before the irradiated chip **compared with the previous**. By  
36 comparing the two irradiation results, thermal neutron's contribution to **the 28 nm** SoC can be  
37 investigated. **Meanwhile, the B and Hf elements'** influence can be analyzed from the irradiation  
38 and the Monte Carlo simulations.

## 39 2. Irradiation Tests

40 The actual atmospheric neutron SEE test is time-consuming, and the spectrum of the  
41 spallation neutron source is the closest to the real one. **Thus**, it is considered the ideal  
42 atmospheric neutron source.<sup>[11]</sup> Scale-down manufacturing technology makes it urgent to  
43 **undertake** more available atmospheric neutron SEE irradiation studies. The China spallation  
44 neutron source **was implemented** in 2018 and made it come true to launch atmospheric neutron  
45 SEE **tests** using a spallation neutron source in China.<sup>[12]</sup> Fig.2 shows the calculated differential  
46 flux of the neutron beam of CSNS (**10<sup>9</sup> of Peking ground**).

47 Based on the CSNS-BL09, two SEE irradiation tests were conducted on the **28 nm** SoC. In  
48 [10], the first irradiation test was performed, and **the** SoC was irradiated by the neutron beam  
49 directly without any shield. In the second irradiation test, **that is the current work, a 2 mm**  
50 Cd slat was placed between the beam ejection stop and **the tested chip** to absorb thermal  
51 neutrons. Fig.3 displays the neutron spectrum at the terminal with and without **the 2 mm** Cd slat  
52 <sup>[8]</sup>. It can be seen that the **2 mm** Cd slat absorbs the neutrons **effectively** whose energies are  
53 below **0.5 eV**.

54 The on-chip memory (OCM) block of the Xilinx Zynq-7000 SoC was tested in two  
55 irradiations. The **64 kB** data in the OCM were tested dynamically. **The check pattern data,**  
56 **0xA5A5A5A5,** were written into the OCM addresses and read back by the SoC, and the SoC  
57 **compared the readback one with the check pattern data to determine whether a SEE took place.**  
58 **The comparison results was moved to PC and refreshed in a terminal. It requires to compare**  
59 **results with the first irradiation, where the normal condition is examined without any**  
60 **mitigation techniques. Hence, the same condition is available in this effort.**

61 **In** both irradiations, the test establishments are the same except the **2 mm** Cd slat. A 2260B  
62 programming DC power supplied the test board. The real-time current was monitored and  
63 recorded by the remote host computer, and the possible single event latch-up was also  
64 investigated. The host computer and the test board communicated through a **universal serial**  
65 **bus** cable, and the running messages were recorded in real-time.

## 66 3. Results and Discussions

67 **Four kinds of soft errors were detected in both irradiations,** including the single bit upset  
68 (SBU), dual cell upset (DCU), multi-cell upset (MCU), and single event functional interruption  
69 (SEFI). No abnormal current was detected, **which** means no latch-up event **emerged** in the **28**  
70 **nm** SoC atmospheric neutron SEE irradiation tests. However, there **are** some **differences**  
71 between the two irradiations **in terms of** SEE cross section. This discrepancy signifies thermal  
72 **neutron impacts the 28 nm SoC** atmospheric neutron SEE.

### 73 3.1. The Detected Events

74 In the second irradiation, 19 events were detected. Table I lists the **number of each type of**  
75 **error**. The number of SBU events is more than others. It is similar to that in the first irradiation.

76 During the second irradiation, the neutron flux above 1 MeV was about  $6.85 \times 10^5 \text{ n} \cdot \text{cm}^{-2} \cdot \text{s}^{-1}$  and  
 77 the corresponding fluence was  $2.47 \times 10^{10} \text{ n} \cdot \text{cm}^{-2}$ . Hence, the SBU cross section is  
 78  $(5.26 \pm 0.26) \times 10^{-10} \text{ cm}^2$  and  $(1.00 \pm 0.05) \times 10^{-15} \text{ cm}^2 \cdot \text{bit}^{-1}$  for the irradiation with few thermal  
 79 neutrons.

80 Table I. The detected SEE in irradiation with few thermal neutrons

SBU	DCU	MCU	SEFI
13	2	2	2

81 Table II. The detected SEE in irradiation with thermal and high energy neutrons.<sup>[10]</sup>

SBU	DCU	MCU	SEFI
21	4	2	5

82  
 83 Table II presents the detected SEE in the first irradiation. It can be seen the number of SBU  
 84 events is 21 in the irradiation, which is also more than others. In Table I and II, it is evident  
 85 that SBU events dominate the detected soft errors in both irradiations.

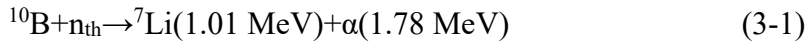
86 Table III presents the SBU cross sections in two irradiations. The neutron fluence of the  
 87 second irradiation is  $2.47 \times 10^{10} \text{ n} \cdot \text{cm}^{-2}$ , higher than that of the first irradiation by 11.26%,  
 88 however, the number of SBU event in the second irradiation is 13 instead of more than 21. This  
 89 phenomenon implies thermal neutron has a contribution to the 28 nm SoC atmospheric neutron  
 90 SEE. The discrepancy between the bit cross sections is  $0.8 \times 10^{-15} \text{ cm}^2 \cdot \text{bit}^{-1}$ . Since the critical  
 91 difference between two irradiations is containing thermal neutron or not, it can be speculated  
 92 thermal neutron causes the discrepancy. It attests the SEE sensitivity of the 28 nm SoC can be  
 93 reduced by about 44.4% by shielding thermal neutron with a 2 mm Cd slat. All these  
 94 demonstrate that risks from thermal neutron cannot be neglected, even though the nanoscale  
 95 chips get rid of BPSG in packages.

96 Table III. The SBU cross sections in two irradiations.

Neutron Beam	Fluence $10^{10} \text{ cm}^{-2}$	SBU	Cross section $10^{-10} \text{ cm}^2$	Bit cross section $10^{-15} \text{ cm}^2 \cdot \text{bit}^{-1}$
CSNS-BL09 <sup>[10]</sup>	2.22	21	$9.46 \pm 0.47$	$1.80 \pm 0.09$
CSNS-BL09+2mm Cd	2.47	13	$5.26 \pm 0.26$	$1.00 \pm 0.05$

### 98 3.2. B Influence

99 The 65 nm MCU atmospheric neutron irradiation results indicated that the secondary  
 100 particles from thermal neutrons interacting with  $^{10}\text{B}$  could result in SEU on advanced electronic  
 101 systems. Compared with the 65 nm memory cell, the SEU critical charge of the 28 nm memory  
 102 cells is lower, and thermal neutron is easier to induce soft errors in the 28 nm process cells.



105 Formulas (3-1) and (3-2) describe the mechanisms of thermal neutron ( $n_{\text{th}}$ ) reacting with  $^{10}\text{B}$ .  
 106 The probability of (3-1) is 6.3%, and that of (3-2) is 93.7%.<sup>[13]</sup> It means the key of thermal  
 107 neutron inducing SEE in the 28 nm SoC is  $^7\text{Li}(0.84 \text{ MeV})$  and  $\alpha(1.47 \text{ MeV})$  particles. They  
 108 deposit energy in the sensitive volumes. Table IV shows the ranges in silicon and the linear  
 109 energy transfers (LETs) of the two secondary particles.<sup>[14]</sup> The ranges in silicon of  $\alpha(1.47 \text{ MeV})$   
 110 and  $^7\text{Li}(0.84 \text{ MeV})$  are just 5  $\mu\text{m}$  and 2.5  $\mu\text{m}$ , which are much less than the thickness of the 28  
 111 nm SoC from top passive layers to substrate's surface.<sup>[15]</sup> This phenomenon preliminarily  
 112 reveals that the B contamination exists inner the chip and approaches sensitive volumes of the

113 SoC. The SEE LET threshold of the 28 nm cell is approximately  $0.50 \text{ MeV}\cdot\text{cm}^2\cdot\text{mg}^{-1}$ .<sup>[16]</sup> For  
 114  ${}^7\text{Li}$ (0.84 MeV) and  $\alpha$ (1.47 MeV), the LETs are  $2.10 \text{ MeV}\cdot\text{cm}^2\cdot\text{mg}^{-1}$  and  $1.15 \text{ MeV}\cdot\text{cm}^2\cdot\text{mg}^{-1}$ ,  
 115 respectively. They are higher than the threshold, which means both secondary particles can  
 116 induce SEE in 28nm SoC.

117 Table IV. The ranges and LETs of secondary particles of  ${}^{10}\text{B}$  with the thermal neutron.

Rang in silicon/ $\mu\text{m}$		LET/ $\text{MeV}\cdot\text{cm}^2\cdot\text{mg}^{-1}$	
${}^7\text{Li}$ (0.84 MeV)	$\alpha$ (1.47 MeV)	${}^7\text{Li}$ (0.84 MeV)	$\alpha$ (1.47 MeV)
2.5	5	2.10	1.15

118 It is different from the 65 nm MCU, the Hf element also exists inner the 28 nm SoC, and the  
 119 cross section of Hf with thermal neutron is even higher than that of silicon. Thus, it cannot  
 120 conclude the difference is induced by  ${}^{10}\text{B}$  directly.

### 121 3.3. Hf Influence

122  ${}^{10}\text{B}$ , in the 28 nm SoC, interacts with thermal neutron inducing SEE, that mainly comes from  
 123 the high probability of nuclear reaction. However, as Fig.4 displays, the primary interaction of  
 124 thermal neutron and the Hf element is the (n,  $\gamma$ ) reaction,<sup>[9]</sup> and the  $\gamma$  rays usually results in  
 125 total ionization dose rather than SEE in the device.<sup>[17]</sup> Because the generated  $\gamma$  rays cannot  
 126 cause SEE directly and have to interact with other atoms to produce secondary heavy ionization  
 127 particles, this possibility is relatively low.

128 Compared with high energy neutrons, cross sections of  ${}^{178}\text{Hf}$  interacting with the eV level  
 129 neutrons even achieve  $10^5$  barns. In this case, whether the hafnium element contributes to 28  
 130 nm SoC atmospheric neutron SEE, required to be comprehensively assessed.

131 In Fig.4, the peak's reaction of  ${}^{178}\text{Hf}$  with several eV neutrons is elastic or (n,  $\gamma$ ). As  
 132 mentioned above, the contribution from (n,  $\gamma$ ) reaction to induce SEE in 28nm SoC is rather  
 133 low. Neutron in elastic interaction can transfer energy to hafnium atoms, it might increase the  
 134 probability of causing SEE. The maximum transfer energy to the Hf atom from neutron can be  
 135 calculated with the formula (3-3).<sup>[18]</sup>

$$136 \quad E_t = \frac{4M_n M_t}{(M_n + M_t)^2} E_n \quad (3-3)$$

137 *E<sub>t</sub> is the max energy transfer to Hf atom with keV, M<sub>n</sub> is the mass of the neutron, which is*  
 138  *$1.67 \times 10^{-27}$  kg, M<sub>t</sub> is the Mass of Hf and it is  $2.96 \times 10^{-25}$  kg, and E<sub>n</sub> is the energy of neutron*  
 139 *with keV.*

140 The current work mainly discusses soft error in the 28 nm SoC induced by thermal neutron  
 141 reacting with the boron and hafnium elements. As stated in Section 2, the neutron with energy  
 142 less than 0.5 eV are absorbed by a 2 mm Cd slat. For the 0.5 eV neutron, the maximum  
 143 transferred energy to Hf atom is about 0.01 eV. Meanwhile, considering the peak elastic cross  
 144 section in Fig. 4, even though it extends the neutron energy to the rightmost peak, the  
 145 corresponding max transferred energies are lower than 0.03 keV. Considering their LETs (the  
 146 corresponding LETs are less than  $0.50 \text{ MeV}\cdot\text{cm}^2\cdot\text{mg}^{-1}$ ), these are all impossible to lead to SEE  
 147 on the SoC. It testifies the high cross section elastic interaction from Hf with thermal and eV  
 148 neutrons does not affect 28nm SoC atmospheric neutron SEE.

149 Hence, it can be concluded the soft error difference between the two irradiations is mainly  
 150 caused by  ${}^{10}\text{B}$ .

### 151 3.4. Monte Carlo Simulation

152 The cut cross section of the chip is investigated and captured, as shown in Fig. 5, the  
 153 thickness and materials of the passive layers were obtained.<sup>[10, 15]</sup> Meanwhile, the 28 nm High-  
 154 k metal gate (HKMG) technology gate contains TiN(8 nm), HfO<sub>2</sub>(10 nm), and SiON(1.2  
 155 nm),<sup>[19]</sup> and the ultra-thin SiON layer can also be an ultra-thin SiO<sub>2</sub> layer in the HKMG

156 technology.<sup>[20]</sup> Relying on these effort and information, two Geant4 Monte Carlo simulation  
 157 models were constructed to examine the Hf element's influence.<sup>[21, 22]</sup> In Fig.6, the TiN and  
 158 ultra-thin SiO<sub>2</sub> layers are considered only in the first model, while the TiN, HfO<sub>2</sub>, and ultra-  
 159 thin SiO<sub>2</sub> layers are considered simultaneously in the second model in Fig.7. Others are the  
 160 same for the two simulation models.

161 The spectrum of neutron sources in the simulation is the same as in the first irradiation test,  
 162 which includes thermal and high energy neutrons. The number of neutrons is 10<sup>7</sup>, and the  
 163 surface area of the model is 10 μm×10 μm. 32×32 sensitive volumes (SVs) are placed, the size  
 164 of the volume is 130 nm×130 nm×130 nm, and the critical charge is 0.18 fC. During the  
 165 simulation, if the deposited energy in an SV overs the critical charge in an EventAction, which  
 166 means an SEU emerged.

167 The number of the upset event in the cells and deposited doses in the ultra-thin SiO<sub>2</sub> layer  
 168 were recorded in both simulations and shown in Table V. It can be seen the number of the upset  
 169 event and the cross section are the same in both simulations. Still, the deposited dose in the  
 170 ultra-thin SiO<sub>2</sub> layers differs by almost 5 times. The simulation results verify that the Hf  
 171 element does not influence 28 nm SoC atmospheric neutron SEE. However, the existence of  
 172 hafnium may increase the total dose risk during atmospheric neutron SEE irradiation. In Fig.4,  
 173 the high (n, γ) cross section also underlines this possible outcomes, because more γ rays means  
 174 more possible total ionization dose risk. And the simulation results is consistent with that. It  
 175 suggests total dose risk monitoring is necessary in much more fluence atmospheric neutron  
 176 SEE irradiation tests for the SoC.

177 Table V. The upset number and deposited doses in two simulations.

Upset number		Bit cross section/cm <sup>2</sup> ·bit <sup>-1</sup>		Deposited Dose/rad	
First Model	Second Model	First Model	Second Model	First Model	Second Model
5	5	5×10 <sup>-16</sup>	5×10 <sup>-16</sup>	12.6	63.3

178 Up to now, we evaluated the 65 nm MCU and 28 nm SoC atmospheric neutron SEE  
 179 depending on CSNS. In the future, more SEE irradiations and assessments will be explored  
 180 further.

#### 181 4. Conclusion

The 28 nm SoC was irradiated twice at CSNS-BL09. In the first irradiation, the spectre  
 covered the thermal and high energy neutron, while thermal neutrons were shielded in the  
 second. The differences in the results were analyzed. The discrepancy between the two  
 irradiation tests is caused by <sup>10</sup>B interacting with thermal neutron. If thermal neutron in the  
 atmospheric environment is shielded by a 2 mm Cd slat, the 28 nm SoC SEE sensitivity can be  
 decreased by 44.4%. The hafnium element does not influence the 28 nm SoC atmospheric  
 neutron SEE, although it also has a high interaction cross section with thermal neutron. The  
 evaluation illustrated attention should be paid to total dose hazard during the 28 nm SoC  
 atmospheric neutron SEE irradiation, since the hafnium element increases the total dose risk.

182

#### 183 Acknowledgment

184 Authors thank the engineers of CSNS-BL09.

185 Project supported by National Natural Science Foundation of China (Grant Nos. 11575138,  
 186 11835006, 11690040, and 11690043)

187

#### 188 References

189 1. R. C. Baumann and E. B. Smith, Neutron-induced 10B fission as a major source of soft

190 errors in high density SRAMs, 2001 Microelectron. Reliab. 41, 211.

191 2. N. Badodekar, Cypress white paper Document, no. 001-88889.

192 3. S. Kumar, S. Agarwal and J. P. Jung, Soft Error Issue and Importance of Low Alpha Solders

193 for Microelectronics Packaging, 2013 Rev. Adv. Mater. Sci. 34, 185-202.

194 4. Chen W, Yang H L and Guo X Q, et al., The research status and challenge of space radiation

195 physics and application, 2017 Chin. Sci. Bull. 62, 978-989.

196 5. T. Yamazaki, T. Kato, T. Uemura, et al., Origin analysis of thermal neutron soft error rate

197 at nanometer scale, 2015 Journal of Vacuum Science & Technology B 33, 020604.

198 6. C. Weulersse, S. Houssany and N. Guibbaud, et al., Contribution of Thermal Neutrons to

199 Soft Error Rate, 2018 IEEE Trans. Nucl. Sci. 65, 1851-1857.

200 7. Y. P. Fang and A. S. Oates, Thermal neutron-induced soft errors in advanced memory and

201 logic devices, 2014 IEEE Trans. Device Mater. Rel. 14, 583-586.

202 8. Z. Hu, W. Yang and Y. Li, et al., Atmospheric neutron single event effect in 65 nm

203 microcontroller units by using CSNS-BL09, 2019 Acta Phys. Sin. 68, 238502.

204 9. Brookhaven National Laboratory, National Nuclear Data

205 Center (NNDC), Evaluated Nuclear Data File (ENDF):

206 <https://www.nndc.bnl.gov/exfor/endl00.jsp>

207 10. W. Yang, Y. Li and Y. Li, et al., Atmospheric Neutron Single Event Effect Test on Xilinx

208 28nm System on Chip at CSNS-BL09. 2019 Microelectron. Reliab. 99, 119-124.

209 11. C. Andreani, R. Senesi and A. Paccagnella, et al., Fast neutron irradiation tests of flash

210 memories used in space environment at the ISIS spallation neutron source, 2018 AIP Adv.

211 8, 025013.

212 12. Y. Chen. China Spallation Neutron Source, 2011 Bulletin of Chinese Academy of Sciences,

213 26, 726-729.

214 13. Tian Y S, Hu Z L and Tong J F, et al., Design of beam shaping assembly based on 3.5 MeV radio-

215 frequency quadrupole proton accelerator for boron neutron capture therapy, 2018 Acta Phys. Sin.

216 67, 142801.

217 14. SRIM (2013). Particle Interactions with Matter [Online]. Available: <http://www.srim.org/>

218 15. W. Yang, Q. Yin and Y. Li, et al., Single-event effects induced by medium-energy protons in 28

219 nm system-on-chip, 2019 Nucl. Sci. Tech. 30, 151.

220 16. M. Amrbar, F. Irom and S. M. Guertin, et al., Heavy ion single event effects measurements of Xilinx

221 Zynq-7000 FPGA, 2015 IEEE Radiat. Effects Data Workshop (REDW), Boston, MA, USA.

222 17. S. D. Mascioia, A. Menicuccia, G. Furano, et al., Towards defining a simplified procedure for COTS

223 system-on-chip TID testing, 2018, Nucl. Eng. Tech., 50, 1298-1305.

224 18. C. Leroy, P. G. Rancoita, Principles of Radiation Interaction in Matter and Detection (2nd Edition),

225 Word Scientific Publishing, 2009.

226 19. S. Uwe, C. S. Hwang, and H. Funakubo. Ferroelectricity in doped hafnium oxide: materials,

227 properties and devices. Woodhead Publishing, 2019.

228 20. M. Czernohorsky, K. Seidel and K. Kühnel, et al. High-K metal gate stacks with ultra-thin

229 interfacial layers formed by low temperature microwave-based plasma oxidation, 2017

230 Microelectron. Eng. 178, 262-265.

231 21. S. Agostinelli, J. Allison, and K. Amako et al., GEANT4-a simulation toolkit, 2003 Nucl. Instrum.

232 Methods Phys. Res. A. 506, 250-303.

233 22. W. Yang, Y. Li, W. Zhang, et al. Electron inducing soft errors in 28 nm system-on-Chip, 2020

234 Radiation Effects and Defects in Solids, 175, 745-754.